

Spectroscopic observation and analysis of plasma turbulence in a Z-pinch

E. A. Oks and V. A. Rantsev-Kartinov

*I. V. Kurchatov Institute of Atomic Energy
and All-Union Research Institute for Physicotechnical and Radio Measurements
(Submitted 11 October 1979)
Zh. Eksp. Teor. Fiz. 79, 99–115 (July 1980)*

The procedure of investigating a turbulent plasma with the aid of the spectral lines of hydrogen is further developed. It is used to analyze the profiles of the lines D_α , D_β , and D_γ emitted in a cylindrical Z-pinch. The observed singularities of the profiles are identified as nonadiabatic Langmuir-noise effects. This has made it possible to determine the plasma concentration by a new method. Lower-frequency electrostatic noise is also observed and its amplitude determined. Polarization measurements give some grounds for assuming that the low-frequency noise comprises Bernstein modes. It is shown that, owing to the anomalous resistance produced by them, the conduction electric field can exceed the induction field and accelerate the ions to observable energies. The theoretically expected peaks in the energy spectrum of the accelerated ions and the time of formation of the accelerated particles also agree with the experimental data.

PACS numbers: 52.35.Ra

1. INTRODUCTION

It is known that in cylindrical Z pinches (CP) with currents $I \sim (2-4) \times 10^5$ A, accelerated deuterons are produced with energies $\mathcal{E} \approx (0.5-3) \times 10^5$ eV,¹ and even higher,² while in noncylindrical pinches, particularly in a plasma focus (PF) with current $I \sim 10^6$ A, deuterons with energies $\mathcal{E} \approx (0.5-4) \times 10^6$ eV are produced (see, e.g., Ref. 3). It appears that such particles are produced as a result of acceleration in high-power electric fields. There are several hypotheses concerning the nature of such fields and the acceleration mechanism (see, e.g., the references in Luk'yanov's book¹ as well as some papers by others⁴⁻⁶). These hypotheses, however, have not been unequivocally confirmed by experiment, and the question still remains open.

The present paper contains an elaboration of the theory of spectroscopic measurements of the parameters of a turbulent plasma: 1) A unified description is presented of the resonant nonadiabatic effects for weak and strong fields. 2) The limits of existence of these effects are determined. 3) A new method of measuring the concentration of a plasma with Langmuir turbulence is described. 4) A method is developed for applying the procedure of Ref. 11 under conditions of insufficient spectral resolution. Results of a spectroscopic investigation of a deuterium plasma in a CP are presented. A detailed analysis of the profiles of the Balmer lines D_α , D_β , and D_γ has made it possible, for the first time ever, to reveal the presence of electrostatic noise (both Langmuir and of lower frequency) and to determine its amplitude. The polarization measurements indicate that the low-frequency noise constitutes apparently Bernstein modes. On this basis it is possible to present a new explanation of the ion-acceleration mechanism, including the experimentally observed limiting energy, the structure of the energy spectrum, and the time of production of the accelerated particles.

2. THEORETICAL BASIS OF PROCEDURE

1. The theory developed in the cited papers⁷⁻¹² is based on separate allowance for the low-frequency (LF)

and high-frequency (HF) electrostatic noise of the plasma. The principal results of these papers consist in the following.

Ion-sound, cyclotron, and other LF noise of the plasma act on the hydrogen atom quasistatically: the profile of the Stark sideband component produced in the transition between the initial (α) and final (β) states is

$$S_{\alpha\beta}(\Delta\lambda) = (I_{\alpha\beta}/C_{\alpha\beta}) W(\Delta\lambda/C_{\alpha\beta}),$$

where $W(F)$ is the distribution function of the LF component F of the electric field of the plasma; the intensities $I_{\alpha\beta}$ and the Stark constants $C_{\alpha\beta}$ were calculated in Ref. 13. For noise with isotropic spectrum, the function $W(F)$ on the integrally significant part agrees (with accuracy not worse than 15%) with the Rayleigh function

$$W_n = \left(\frac{6}{\pi}\right)^{1/2} \frac{3F^2}{F_0^3} \exp\left(-\frac{3F^2}{2F_0^2}\right)$$

under the condition $F_0 \gtrsim 10eN^{2/3}$, where F_0 is the mean squared field of the LF noise and N is the plasma concentration.

Under the influence of the HF Langmuir noise, the half-width¹⁾ of a line with an intensive central component increases by an amount

$$\Delta\lambda_{1/2}^{\text{HF}} \approx 4\gamma_p (e_\alpha^2 + e_\beta^2) \lambda_p \omega_p^{-2}, \quad (1)$$

where

$$e_\nu = (3/32)^{1/2} n_\nu g_\nu (me)^{-1} \hbar E_0, \quad g = [n_\nu^2 - (n_1 - n_2)^2 - m_\nu^2 - 1]^{1/2}; \quad (2)$$

here ω_p is the plasma frequency, $2\gamma_p$ is the half-width of the frequency spectrum of the noise, E_0 is the mean squared noise amplitude; $\lambda_p = \omega_p \lambda_{\alpha\beta}^2 / 2\pi c$, $\lambda_{\alpha\beta}$ is the unperturbed wavelength; $n_{1\nu}$, $n_{2\nu}$, m_ν are the parabolic quantum numbers of the initial ($\nu = \alpha$) or final ($\nu = \beta$) states, n_ν is the principal quantum number, m is the electron mass, and e is its charge. However, the principal effect (of lower order in the parameter $e_\nu/\omega_p \ll 1$) of the action of the Langmuir noise is two groups of dips, which can appear at the following distances from the line center:

$$\lambda_\alpha = n_\alpha^{-1} X_{\alpha\beta} \lambda_\beta, \quad \lambda_\beta = n_\beta^{-1} X_{\alpha\beta} \lambda_\alpha, \quad (3)$$

where²⁾ $X_{\alpha\beta} \equiv n_\alpha(n_1 - n_2)_\alpha - n_\beta(n_1 - n_2)_\beta$. This leads to the characteristic chopped-up profiles of the hydrogen lines. Such profiles of the lines H_α , H_β , H_γ , and H_δ are observed in many experiments for various methods of production, containment, and turbulization of the plasma, and are analyzed in Ref. 11. In all cases, good agreement with formula (3) was established. In the present investigation of the Z pinch, we registered likewise jagged profiles of the deuterium lines D_α , D_β , and D_γ (see Figs. 4-7).

2. The appearance of the resonant nonadiabatic effects that manifest themselves as ν -dips ($\nu = \alpha, \beta$) is due to the group of atoms that experiences the action of the static field

$$F_\nu = (3\hbar n_\nu)^{-1} 2m\epsilon\omega_p \quad (\nu = \alpha, \beta). \quad (4)$$

In the field F_ν , the frequency distance $\omega_F^{(\nu)} = 3n\hbar F/2me$ between $2n_\nu - 1$ equidistant Stark sublevels of the ν -multiplet becomes equal to ω_p . The mechanisms of dip formation are substantially different in the cases of small ($\epsilon_\nu \ll \gamma_p$) and large ($\epsilon_\nu \gg \gamma_p$) HF noise fields.

In the case of weak fields, $\epsilon_\nu \ll \gamma_p$, the principal role is played by the resonant dependence of the width of the Stark sublevels

$$\Gamma_\nu \approx \epsilon_\nu^2 \gamma_p / [\gamma_p^2 + (\omega_F^{(\nu)} - \omega_p)^2],$$

which is governed by the HF noise, on the detuning $(\omega_F^{(\nu)} - \omega_p)$. At resonance we have

$$\Gamma_\nu^{res} \approx \epsilon_\nu^2 / \gamma_p,$$

and off resonance (e.g., at $\omega_F^{(\nu)} \ll \omega_p$)

$$\Gamma_\nu \approx \epsilon_\nu^2 \gamma_p / \omega_p^2 \approx (\gamma_p / \omega_p)^2 \Gamma_\nu^{res} \ll \Gamma_\nu^{res}.$$

Therefore the resonant atom emit a broader Lorentz profile, and hence less intense at its center, than the nonresonant atoms. This lowering of the intensity (dips) on the profile of each sideband component will be encountered twice, corresponding to the fields F_α and F_β of Eq. (4). Each dip is flanked by two intensity rises (hills). The distance from the dip to the hill is equal to the half-width of the dip and amounts to

$$(\Delta\omega_{1/2}^{dip})_\nu \sim \gamma_p^{1/2} (X_{\alpha\beta} \epsilon_\nu / n_\nu)^{1/2}.$$

However, the relative depth of these dips is small

$$(\Delta S/S)_\nu \sim (n_\nu / X_{\alpha\beta}) (\epsilon_\nu / \gamma_p)^2 \ll 1$$

(see Fig. 1).

In the case of strong fields, $\epsilon_\nu < \epsilon_p$, the HF width of the Stark sublevels saturates and reveals no resonant absorption: $\Gamma_\nu = \gamma_p$ at all detunings $\omega_F^{(\nu)} - \omega_p$ smaller than ϵ_ν . At $\epsilon_\nu \gg \gamma_p$, however, the stochastic character of the HF noise does not appear within the characteristic times of variation of the probability P_ν that the atom is at the sublevel ν . This has made it possible to employ in Ref. 11 a method similar to the Rabi "rotating wave" approximation known from quantum optics,¹⁴ and to obtain an analytic solution that is not restricted by perturbation theory (in contrast to the preceding study⁸). It turned out that the probability P_ν oscillates at the Rabi frequency, which, in particular at $\omega_F^{(\nu)} - \omega_p = 0$, is

equal to ϵ_ν .

This result likewise admits a simple interpretation in terms of the quasienergy states (QES). In fact, the $(2n_\nu - 1)$ Stark sublevels are so arranged that the matrix elements of the dipole moment differ from zero only for transitions between neighboring sublevels that differ in frequency by $\omega_F^{(\nu)}$. In the case $\omega_p = \omega_F^{(\nu)}$, degeneracy of the QES is produced in the noninteracting atom + field system. When account is taken of the dipole interaction, the degenerate QES are repelled from one another in frequency by $2\epsilon_\nu$. The radiation intensity at the frequencies $\omega_\nu \equiv X_{\alpha\beta} \omega_p / n_\nu$ decreases abruptly, and at the frequencies $X_{\alpha\beta}(\omega_p \pm \epsilon_\nu) / n_\nu$ it increases; dips flanked by hills appear and have a larger relative depth $(\Delta S/S)_\nu \approx n_\nu / X_{\alpha\beta} \sim 1$ and a half-width $(\Delta\omega_{1/2})_\nu = X_{\alpha\beta} \epsilon_\nu / n_\nu$ (see Fig. 1).

We note that prior to the publication of our papers^{8,11} it was assumed that the plasma oscillations can lead to a single spectroscopic effect, namely to the appearance of satellite hills due to adiabatic effects.^{15,16} The dips predicted by us^{8,11} are a fundamentally new effect in plasma spectroscopy.³⁾

Deep dips (and high hills) on the deuterium line of the investigated Z pinch (see Figs. 4-7), just as those on the hydrogen lines and analyzed by us earlier,¹¹ correspond to the case of strong fields $\epsilon_\nu \gg \epsilon_p$. In the wavelength scale, the half-widths of the dips are then

$$(\Delta\lambda_{1/2}^{dip})_\nu = (\epsilon_\nu \omega_p^{-1}) \lambda_\nu, \quad (5)$$

where the positions of the dips λ_ν are determined by Eq. (3).

3. The solution in our paper,¹¹ just as the Rabi solution,¹⁴ has an upper bound on the value of the HF field. Dips exist under the condition $E_0 / \sqrt{2} \ll F_\nu$, i.e., at

$$E_0 \ll E_c(n) = (3n\hbar)^{-1} 2^{1/2} m\epsilon\omega_p. \quad (6)$$

The critical value of the ratio of the densities of the HF noise energy and the thermal energy is

$$\xi_c = E_c^2(n) / 8\pi NT_e = 8I / 9n^2 T_e,$$

where I is the hydrogen ionization potential and T_e is the electron temperature. Consequently, if the critical energy of the plasma electrons exceeds the binding energy of the atomic electron, the conditions for the existence of dips (6) is more stringent than the "usual" restriction $E_0 \lesssim (8\pi NT_e)^{1/2}$.

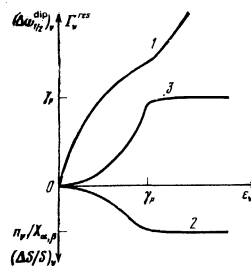


FIG. 1. Dependence of the half-width $(\Delta\omega_{1/2}^{dip})_\nu$, of their relative depths $(\Delta S/S)_\nu$, (curve 2), and of the width of the Stark sublevels $\Gamma_\nu^{res} \equiv \Gamma_\nu(\omega_F = \omega_p)$, due to the HF noise (curve 3) on the reduced HF noise field intensity ϵ_ν (see the explanation in the text, item 2 of Sec. 2).

4. The dips can be used not only for the measurement of the HF field [by means of Eq. (5)], but primarily as a new independent method of measuring the concentration of a plasma with Langmuir turbulence. The gist of the method consists in the fact that the relative distances of the dips from the center of the considered hydrogen line (e.g., in units of λ_p) make up a definite set of rational numbers ($X_{\alpha\beta}/n_\alpha, X_{\alpha\beta}/n_\beta$), which is unique for this line only. Comparing the relative distances of the decreases of the intensity, observed in the spectral lines, with this set of numbers it is possible to draw conclusions concerning the nature of these decreases. If they agree well, they are due to Langmuir noise and then, by measuring the absolute distances between the dips and the line center, it is possible to determine λ_p , and then the plasma concentration, using the formula

$$N = \pi m c^2 e^2 \lambda_{\alpha\beta}^{-4} \lambda_p^{-2}. \quad (7)$$

If the spectral resolution is insufficient, some part of the dips cannot be registered and the experimentally obtained set of numbers λ_p/λ_p will be less numerous than the theoretical set, making the identification difficult. It is convenient in this case to distinguish beforehand in the theoretical set reference dips having the largest equivalent width w_p , which can be determined from the formula

$$w_p = \int_{\lambda_p - \delta\lambda_p}^{\lambda_p + \delta\lambda_p} d(\Delta\lambda) [S_0(\Delta\lambda) - S(\Delta\lambda)], \quad \delta\lambda_p = (\Delta\lambda_{\text{th}}^{\text{dip}})_p,$$

where $S_0(\Delta\lambda)$ is the line profile unperturbed by the HF noise. Calculation shows that

$$w_p = \epsilon_p \frac{I_{\alpha\beta}}{C_{\alpha\beta}} W \left(\frac{\lambda_p}{C_{\alpha\beta}} \right) \frac{\lambda_{\alpha\beta}^2}{2\pi c} \propto \frac{I_{\alpha\beta}}{X_{\alpha\beta}} n_p g_p = f_p. \quad (8)$$

The quantities f_p , which are independent of the plasma parameters determine the ratios of the equivalent widths within each of the two groups (α or β) of dips: $w_{\alpha'}/w_\alpha = f_{\alpha'}/f_\alpha$, $w_{\beta'}/w_\beta = f_{\beta'}/f_\beta$.

Figure 2 indicates the theoretically expected positions of the reference dips on the profiles of H_α , H_β , and H_γ .

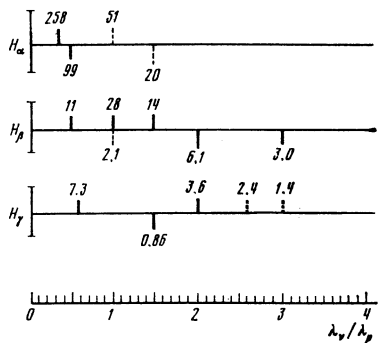


FIG. 2. Theoretically expected positions of the reference dips on the profiles of the lines D_α , D_β and D_γ . The dips produced on account of the resonance between ω_p and the splitting of the upper multiplet with $n_\alpha > 2$ (α -group) are indicated by vertical lines above the abscissa axis. The dips produced on account of the resonance between ω_p and the splitting of the lower multiplet with $n_\beta = 2$ (β -group) are indicated by vertical lines under the abscissa axis. Alongside the lines is shown the equivalent dip width w_p in relative units [see Eq. (8)]. Solid lines indicate dips for which $w_\alpha > w_{\alpha \text{ max}}/2$ and $w_\beta > w_{\beta \text{ max}}/2$. The dashed lines in the α and β groups indicate the broadest of the remaining dips.

and gives the calculated values of f_p , multiplied for convenience by 100.

The ratios w_α/w_β of the equivalent widths of the dips from different groups depend on the plasma concentration and on the form of the function $W(f)$:

$$w_\alpha/w_\beta = f_\alpha W(F_\alpha)/f_\beta W(F_\beta).$$

3. APPARATUS AND MEASUREMENT METHODS

In this experiment, the plasma source was a cylindrical Z pinch for the following reasons. First, the plasma column had cylindrical symmetry, and the variation of the parameters relative to φ can be neglected in the macroscopic treatment. Second, the electrodes are far from the observation zone and have therefore no effect on the plasma parameters. Third, this type of installation reproduces well the discharges if the initial conditions are the same. Furthermore, the geometry of the CP is such that spectral information can be relatively easily obtained from the discharge.

The chamber of the apparatus was made of aluminum to decrease the influence of the impurities, and had an inside diameter $D=2$ cm and a length $L=70$ cm. Flat copper electrodes were placed 60 cm apart and covered the entire cross section of the chamber. Four diagnostic openings of diameter $d=30$ mm were made in the equatorial plane. The pulsed discharge was fed from a low-inductance bank with a total capacitance $60 \mu\text{F}$, on which the working voltage was 30 kV. The maximum discharge current reached $I_{\text{max}}=350-400$ kA, with $I(t) \approx 200$ kA and $I(t_{\text{II}}) \approx 300$ kA at the instants of the first and second singularities, respectively. The current rise time to the maximum was $4.5 \mu\text{sec}$. The maximum value of the time derivative of the current was in this case $\dot{I}_{\text{max}} \approx 4 \times 10^{11}$ A/sec.

The placement of the measurement apparatus is shown in Fig. 3. A "Yupiter-3" lens 7 was placed on the window 6. The lens was covered with light filters 13 that separated the investigated line and with an organic polarization light filter 12. The geometry of the setup made it possible to project with the aid of this lens a volume $\sim 0.7 \text{ cm}^3$ at the center of the chamber onto the

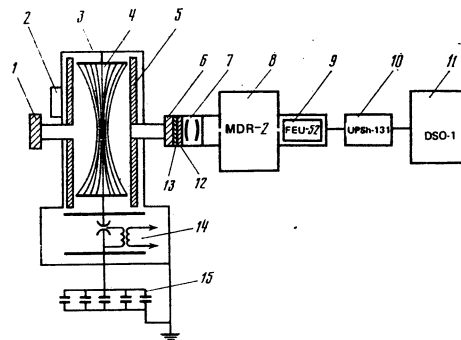


FIG. 3. Experimental setup: 1—window, 2—integral neutron counter, 3—coaxial return lead, 4—plasma, 5—aluminum chamber, 6—window, 7—"Yupiter-3" lens ($F=5$ cm, relative aperture 1:1.5), 8—MDR-2 monochromator, 9—FEU-52A photomultiplier, 10—broadband preamplifier UPSh-130, 11—DSO-1 oscilloscope, 12—polarization light filter, 13—light filter for the investigated line, 14—coaxial discharge gap with igniter, 15—capacitor bank $C=60 \mu\text{F}$, $U=30$ kV.

plane of the entrance slit of the monochromator. The radiation separated by the monochromator 8 was incident on the photocathode of an FEU-52A photomultiplier, whose signal was applied through preamplifier UPSh-130 to a DSO-1 oscilloscope. This measurement system produced a minimum induced noise, an important factor in the measurements of fast processes.

In the previously described experiments with the same setup^{18,19} it was shown, in particular, that if the chamber was well preconditioned (to a residual pressure $\leq 5 \times 10^{-7}$ Torr) and if the initial conditions were identical, then the scatter of the signal amplitude (and hence of the plasma parameters N and T_e) was $\sim 10\%$. This was evidence of the possibility of recording the profiles of the spectral lines point by point with accumulation of statistics from discharge to discharge. At the initial stage of the present experiments, 20–25 discharges were produced at each position of the monochromator drum, to determine the scatter. It turned out that it has the same value, $\sim 10\%$. Subsequently the results of the measurements at each value of $\Delta\lambda$ were averaged over 3–5 discharges.

The width of the entrance and exit slits of the monochromator in measurements with the D_α line were $30 \mu\text{m}$, corresponding to a spectral resolution $\approx 1.2 \text{ \AA}$. To register the lines D_β and D_γ , a different diffraction grating was used, and the slits were $20 \mu\text{m}$ wide, so that the spectral resolution was $\approx 0.4 \text{ \AA}$.

The measurement apparatus was carefully screened against electromagnetic induction. Its temporal resolution ($\sim 20 \text{ nsec}$) made it possible to relate the recorded radiation with the various phases of the discharge.

4. ANALYSIS OF MEASUREMENT RESULTS

1. Typical profiles of the Balmer lines D_α , D_β , and D_γ registered during different phases of the discharge are shown in Figs. 4–7. The principal characteristic feature of all the profiles is their jaggedness: in each wing there are observed several intensity dips, and sometimes almost down to zero value. Let us see what

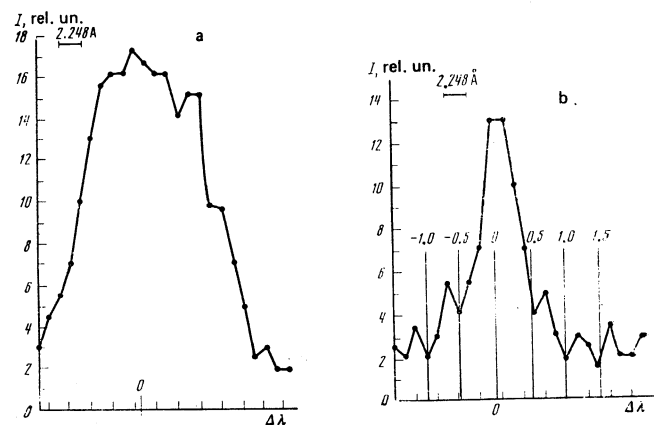


FIG. 4. Registered profiles of the D_α line at a pressure $P_0 = 0.15$ Torr: a—at the instant of the first singularity; b—after the instant of the second singularity. The vertical line segments indicate the theoretically expected positions of the dips. The segments are marked by the distances of the dips from the center of the line in units of λ_p [see formula (3)].

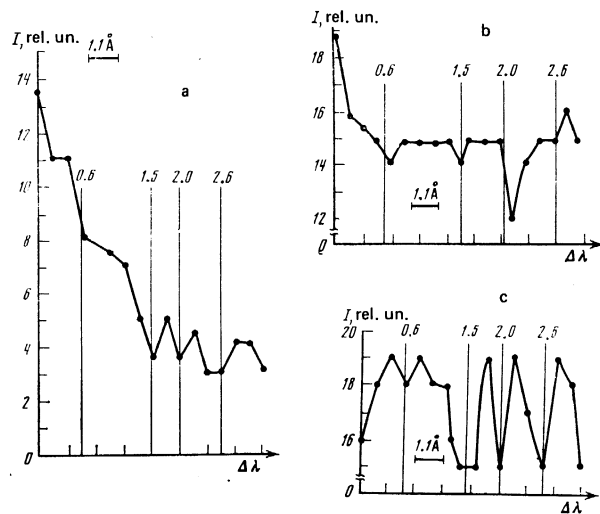


FIG. 5. Registered profiles of the lines D_γ at a pressure $P_0 = 0.15$ Torr: a—at the instant of the first singularity; b—at the instant of the first singularity; c—between the instants of the first and second singularities. The vertical lines and the numbers above them denote same as in Fig. 4.

effects can account for the observed singularities.

The magnetic field of the discharge current is $H = 2I/cr \leq 10^5$ Oe, since the observed radius of the pinch is $r \geq 1 \text{ cm}$. In such fields, the quadratic Zeeman effect on the lines D_α , D_β , and D_γ is small compared with the linear one, so that only triplet magnetic splitting is possible. Consequently, the observed number of peaks (on the order of ten on the profiles D_β and D_γ) cannot be attributed to the Zeeman effect.

To explain the observed number of peaks we can propose that low-frequency electric fields are excited in the plasma, and the distribution $W(F)$ of their amplitudes is for some reason much narrower than a Rayleigh distribution, and the field F can be regarded as quasi-homogeneous. But in this case the half-width of the Stark component

$$(\Delta\lambda_{1/2})_{\alpha\beta} = C_{\alpha\beta} \Delta F_{1/2}^{(W)}$$

[$\Delta F_{1/2}^{(W)}$ is the half-width of the $W(F)$ distribution] is proportional to its distance from the center of the line.

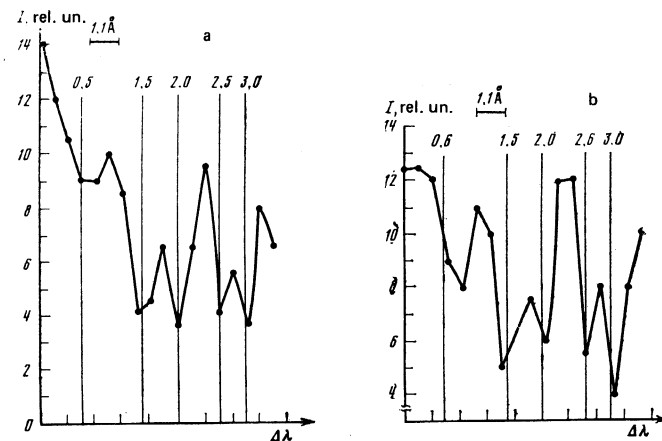


FIG. 6. Registered profiles of the line D_γ at a pressure $P_0 = 0.085$ Torr: a—at the instant of the first singularity; b—between the instants of the first and second singularities. The vertical lines and the numbers above them denote the same as in Fig. 4.

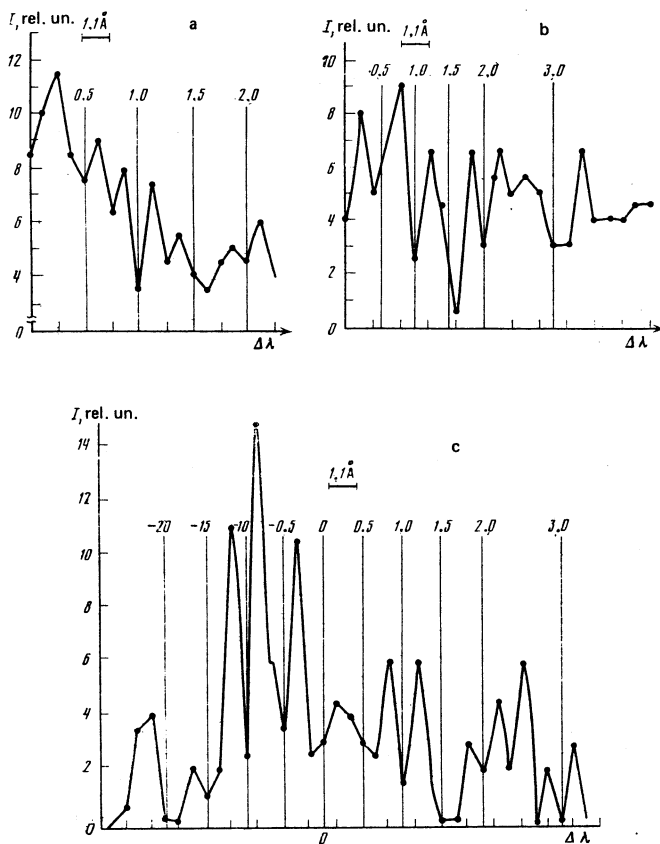


FIG. 7. Registered profiles of the line D_β at a pressure $P_0 = 0.15$ Torr: a—at the instant of the first singularity; b—before the instant of the second singularity; c—after the instant of the second singularity (both wings are shown, since the profile is greatly asymmetrical). The vertical lines and the numbers above them denote the same as in Fig. 4.

Therefore on going farther into the wing the resolution of the individual components should become worse, in contradiction to the observed profiles.⁴⁾

Finally, assume that HF Langmuir (quasimonochromatic) oscillations of frequency ω_p are excited in the plasma. If for some reason the principal (nonadiabatic) effect of the action of the HF noise, described in Sec. 2, could not appear, then their role would reduce to adiabatic satellites at distances $\lambda_{ab} + k\lambda_p$, where $k = \pm 1, \pm 2, \dots$ ^{15,16} This, however, contradicts the observed peak distribution, which is not equidistant (especially on the D_γ line).⁵⁾

Thus, it remains to check the possibility of attributing the observed structure of the profiles to the principal resonant effect of the action of the HF noise, as will in fact be done below.

2. Comparison of the relative distances of the observed dips from the line center with the theoretically expected relative positions of the reference dips (see Fig. 2) shows good agreement for all the profiles of the lines D_α , D_β , and D_γ at our disposal. In particular, for the typical profiles of D_α , D_β , and D_γ presented above this can be verified from an examination of Figs. 4–7, which show the theoretical positions of the dips (now already in absolute scale). This agreement for a large number of profiles of different Balmer lines can hardly be accidental, the more so, e.g., since on the D_γ pro-

file the dips are not equidistant (their distances from the center are $\frac{3}{5}\lambda_p, \frac{3}{2}\lambda_p, 2\lambda_p, \frac{13}{5}\lambda_p$).

From the absolute positions of the observed dips we obtain for each line the value of λ_p , and then the plasma concentration N by means of formula (7). It turns out that for profiles pertaining to one and the same discharge phase (e.g., at the instant of the first singularity), the experimentally measured λ_p decreases on going from D_α to D_β and D_γ , with $\lambda_p \propto \lambda_{ab}^2$, so that all three Balmer lines give the same value of N . This is additional evidence of the reliable identification of the measured dips with the predicted ones.

Most experiments were formed at a molecular deuterium pressure $P_0 = 0.15$ Torr. At the instant of the first singularity, the measurement of the plasma concentration by the indicated method in accord with D_α , D_β and D_γ yields $N \approx 4 \times 10^{15} \text{ cm}^{-3}$. As a control, experiments were performed also at a lower pressure $P'_0 = 0.085$ Torr (See Fig. 6). The relative positions of the dips on the profile of D_γ remained the same, and the absolute distances of the dips from the line center decreased, so that measurements relative to these lines yielded $N' \approx 2 \times 10^{15} \text{ cm}^{-3}$. The ratio $N/N' = 2$ is in accord (within the limits of the error of the method) with the ratio $P_0/P'_0 \approx 1.8$, and this again indicates that the experimental data have been correctly interpreted theoretically.⁶⁾

3. It is of interest to compare the obtained value of the plasma concentration (on the periphery of the pinch) at the instant of the first singularity, $4 \times 10^{15} \text{ cm}^{-3}$, with the value obtained from an analysis of the half-widths of the profiles.

It was shown in a preceding paper²⁵ that from the theoretical point of view, in the absence of noise, the dominant broadening mechanism under the conditions of the present experiment is the impact action of the ions. In this case, the measured half-width of the line $D_\beta[\Delta\lambda_{1/2}(D_\beta) \approx 10 \text{ \AA}]$ at the instant t_1 corresponds to $N > N_{\min} \approx 1.0 \times 10^6 \text{ cm}^{-3}$.²⁵

The substantially higher concentration obtained from $\Delta\lambda_{1/2}(D_\beta)$ indicates that intense low-frequency noise develops in the plasma; since the D_β line does not have a central Stark component, the quasistatic action of the

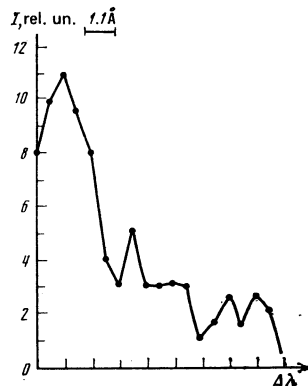


FIG. 8. Registered polarization profile of the D_β line at a pressure $P_0 = 0.15$ Torr at the instant of the first singularity. The polaroid transmission axis is oriented perpendicular to the axis of the installation.

low-frequency noise with a mean-squared field F_0 increases $\Delta\lambda_{1/2}^{\text{exp}}(D_\beta)$ to a value (Ref. 9)⁷⁾

$$\Delta\lambda_{1/2}^{\text{theor}}(D_\beta) \approx 0.2F_0. \quad (9)$$

Substituting $\Delta\lambda_{1/2}^{\text{exp}}(D_\beta) \approx 10 \text{ \AA}$, we get $F_0 \approx 50 \text{ kV/cm}$.

The fact that the Stark broadening of the line is due to collective low-frequency fields and not to random thermal motion of the ions is confirmed also by polarization experiments. In these experiments the polaroid transmission axis was perpendicular to the axis of the apparatus. An elementary analysis of the polarization of the light within the Stark profile shows that the ratio of the half widths $\Delta\lambda_{1/2}^{\text{pol}}$ and $\Delta\lambda_{1/2}^{\text{unpol}}$ of the polarized and unpolarized profiles of the line D_β should amount in this experiment to

$$\eta = \frac{\Delta\lambda_{1/2}^{\text{pol}}}{\Delta\lambda_{1/2}^{\text{unpol}}} \approx \frac{F_\phi^2 + F_z^2}{F_\phi^2 + F_z^2 + 2F_z^2}. \quad (10)$$

(the z axis of the cylindrical coordinate system is directed along the current, and the ϕ axis along the magnetic field of the current).⁸⁾ In particular, one should expect $\eta \approx 3^{-1/2}$ in the case $F_\phi^2 \ll F_z^2 \approx F_\phi^2$ and $\eta \approx 3^{-1/2}$ in the case $F_z^2 \gg \max(F_\phi^2, F_z^2)$.

A typical form of the polarization profile of the D_β line is shown in Fig. 8. The measured value $\Delta\lambda_{1/2}^{\text{pol}} \approx 6 \text{ \AA}$ (i.e., $\eta \approx 0.6$) is evidence of anisotropy of the low-frequency fields and corresponds best to the case $F_\phi^2 \ll F_z^2 \approx F_\phi^2$.

4. In the time interval between the first (t_I) and second (t_{II}) singularities, owing to the considerable line broadening, an exact measurement of $\Delta\lambda_{1/2}(D_\beta)$ is impossible. It can only be estimated by the inequality $\Delta\lambda_{1/2}(D_\beta) > 10 \text{ \AA}$, from which it follows [see Eq. (9)] that $F_0 > 50 \text{ kV/cm}$. The line profiles undergo simultaneously the following changes: The hills that flank each dip in accordance with the theory, begin to grow in intensity, and when the instant t_{II} is approached the most intensive hill becomes noticeably closer to the line center (Fig. 7b). This indicates that the distribution function $W(F)$ becomes narrower, since the intensity of the hill near the dip on the wavelength is proportional to $W(\lambda_\nu/C_{\alpha\beta})$.

After the instant t_{II} , the two most intense hills (one in each line wing) exceed the remaining ones so much that the quantity $\Delta\lambda_{1/2}(D_\beta)$ can be approximately estimated from the distance between them (Fig. 7c).⁹⁾ It amounts to $\approx 5.5 \text{ \AA}$, and $\Delta\lambda_{1/2} \approx (7-8) \text{ \AA}$, so that $F_0 \sim 40 \text{ kV/cm}$.

We emphasize that the values $F_0 \sim 50 \text{ kV/cm}$ and $N \sim 4 \times 10^{15} \text{ cm}^{-3}$ measured at the instant t_I pertain to the periphery of the pinch (it follows from laser-scattering experiments¹⁸ that N at the center of the pinch can be larger by one and one-half or two orders of magnitude). Assuming that at the instant t_I we have in accordance with Ref. 18 $T_i \geq 30 \text{ eV}$ and $T_e \lesssim T_i$, we find that the turbulence level is $\xi \lesssim 10^{-2}$.

The obtained values $F_0 \sim 50 \text{ kV/cm}$ make it possible to obtain the upper bound of the characteristic frequency Ω of the low frequency noise from the condition that they be quasistatic:

$$\Omega \ll \frac{3nhF}{2me} \sim 10^{12} \text{ sec}^{-1} < \omega_p (N=4 \cdot 10^{15} \text{ cm}^{-3}) \approx 3.6 \cdot 10^{12} \text{ sec}^{-1}.$$

5. In accordance with formulas (2), (3), and (5), we can determine from the measured half-widths of the dips ($\Delta\lambda_{1/2}^{\text{dip}}$) the mean squared amplitude E_0 of the HF noise:

$$E_0 = B(g_\nu X_{\alpha\beta})^{-1} (\Delta\lambda_{1/2}^{\text{dip}})_\nu, \quad (11)$$

where $B(D_\alpha) \approx 176$ and $B(D_\beta) \approx 322$. It is best to measure the values of $(\Delta\lambda_{1/2}^{\text{dip}})_\nu$ for the reference dips that are farthest from the line center, since they are broader than the dips closer to the center. Substituting the measured $(\Delta\lambda_{1/2}^{\text{dip}})_\nu$ of these dips on the lines D_α and D_β in (11), we find that $E_0(t_I) \sim 50-80 \text{ kV/cm}$. The large measurement error is due to the insufficient spectral resolution.

6. At the instant t_{II} the value of $\Delta\lambda_{1/2}(D_\alpha)$ reaches 15.7 \AA (Fig. 4, curve a), and decreases in succeeding instants of time (Fig. 4, curve b). We show first that the "laminar" (unconnected with the turbulence) broadening mechanisms in a plasma with parameters $T_e(t_I) \approx T_i(t_I) \geq 30 \text{ eV}$ and $N \approx 4 \times 10^{15} \text{ cm}^{-2}$ cannot explain the measured value of $\Delta\lambda_{1/2}(D_\alpha)$.

For the D_α line, the ion impact half-width is $(\Delta\lambda_{1/2})_{\text{imp}}^{(i)} < 4 \text{ \AA}$. The Doppler half-width D_α can reach 15.7 \AA only at $T_e \approx 2 \text{ keV}$, in contradiction to the upper bound $T_e \lesssim 10^2 \text{ eV}$ obtained in the preceding experiments.¹⁸ The contribution of the remaining broadening mechanisms in a "laminar" plasma having the indicated parameters can be neglected.

It was shown earlier²⁵ that the "anomalous" value of $\Delta\lambda_{1/2}(D_\alpha)$ cannot be attributed also to self-absorption. Thus, to explain the value of $\Delta\lambda_{1/2}(D_\alpha)$ we must resort to "turbulent" broadening mechanisms, among which the principal role for the D_α line should be played by the broadening by HF noise [see formulas (1) and (2)]. For the D_α line formula (1) takes the form $\Delta\lambda_{1/2}^{\text{HI}} \lesssim 5\gamma/\omega_p < 5 \text{ \AA}$, so that at the values of N and E_0 indicated above we have $\Delta\lambda_{1/2}^{\text{eff}} \lesssim 5\gamma/\omega_p < 5 \text{ \AA}$. Formula (1), however, was obtained under the assumption $F \gg E_{\text{eff}} = E_0/\sqrt{2}$. In the considered case, most atoms radiate under conditions $F \lesssim E_{\text{eff}}$. The half-width of the line can then reach the value

$$(\Delta\lambda_{1/2}^{\text{HF}})_{\text{max}} \approx 2\lambda_p. \quad (12)$$

Substituting in (12) the measured $\Delta\lambda_{1/2}(D_\alpha) = 15.7 \text{ \AA}$, we get λ_p and the plasma concentration in accord with formula (7). The value $N \approx 4 \times 10^{15} \text{ cm}^{-3}$ obtained in this manner agrees with the value obtained above by measuring the positions of the dips on the D_α , D_β and D_γ profiles. This attests one more to the adequacy of the theoretical interpretation of the experimental data.

The decrease of $\Delta\lambda_{1/2}(D_\alpha)$ after the instant t_I can be attributed to the increase of the ratio F_0/E_0 , as a result of which the fraction of the atoms that radiate under conditions $F \lesssim E_{\text{eff}}$ is decreased.

5. CURRENT INSTABILITIES AND THE PARTICLE ACCELERATION MECHANISM

The paper of Vikhrev and Korzhavin²⁶ contains a table of the principal types of current instabilities that can

be responsible for the appearance of the anomalous resistance in Z pinches. Judging from this table, the directivity pattern of the low-frequency noise, observed in the presented experiment ($F_0^2 \lesssim F_e^2 \approx F_0^2$), gives some grounds for assuming that the LF noise constitutes Bernstein modes.¹⁰ The Stark broadening of the Balmer line D_n by Bernstein modes is quasistatic if the oscillation frequency in the laboratory frame is

$$\omega_{lab} = (\omega_{He} - \mathbf{k}\mathbf{u}) \sim \omega_{He} v_{Ti} / 2me \ll 3\pi h F_0 / 2me$$

(here \mathbf{u} is the current velocity; $\omega_{He} = eH/mc$). Under the conditions of the present experiment the last inequality is numerically equivalent to the inequality $nu/v_{Ti} \gg 1$, i.e., it is already satisfied at $u \gtrsim v_{He}$.

In the saturation state, the density of the electrostatic energy of the Bernstein modes should amount according to theoretical estimates to $\sim (\omega_{He}/\omega_p)^2 (u/v_{Ti})^3 NT_e$,²⁸ corresponding to a field $F_0^{\text{theor}} \sim 10^{-4} IT^{1/2}/r$. Under the conditions of the present experiment we have $F_0^{\text{theor}} \sim \text{kV/cm}$, which agrees with the measured values $F_0^{\text{theor}} \sim 50 \text{ kV/cm}$.

In the existing calculations of the dynamics of the Z pinch, the anomalous resistance was either not taken into account (e.g., in Ref. 21), or was assumed to be due to ion-sound^{29,30} or electron-sound²⁶ instabilities. This has raised difficulties in the explanation of the particle acceleration mechanism. Thus, according to an MHD calculation,³¹ the electric induction field $E_z^{\text{ind}} = -v_r H/c \sim v H/c$ can produce in the neck region, even if account is taken of the plasma leakage, only a potential difference $\Phi_e \lesssim 250 \text{ kV}$ for CP and $\Phi_e \lesssim 900 \text{ kV}$ for a PF. However, first, in the experiments of Refs. 2 and 3 the particles observed have much higher energies and, second, the acceleration of the ions over the length of the neck in a field $E_z^{\text{ind}} \ll H$ is possible only under the condition $r < v_{Ti}/\omega_{Hi} \equiv \rho_{Ti}$, when the MHD calculation cannot be used.¹¹ A kinetic calculation for the PF conditions³⁰ have shown that compressions down to $r < \rho_{Hi}$ does not take place, and the superthermal ions have velocities $v_i \sim (3-5) v_{Ti}$, corresponding to energies $\mathcal{E} \lesssim 10^5 \text{ eV}$, insufficient to explain the experimental results of Ref. 3.

The Bernstein modes increase the collision frequency to $\nu_{\text{eff}} \sim (u/v_{Te})^3 \omega_{He}$,²⁸ so that the conduction field

$$E_z^{\text{cond}} = -m\nu v_{Ti} / e \sim H u^2 / c v_{Te}^3$$

can exceed E_z^{ind} at $u \gtrsim v_{Te} (m/M)^{1/8} \equiv u_1$. It is important that in this case the displacement of the deuteron across the magnetic field is not limited to the value ρ_{Hi} : the deuterons can be displaced by a distance $2E_z Mc^2 / eH^2 \equiv L > \rho_{Hi}$, and acquire an energy $2Mc^2 (E_z/H)^2 \equiv \mathcal{E}_L$ (see, e.g., Ref. 32). To go over into the acceleration regime it suffices to decrease the radius of the neck to values $r < L$ (and not to values $r < \rho_{Hi}$ as was required in the previously proposed theoretical models).

When the equality $H = 2I/cr$ is taken into account, the condition $r < L$ takes the form

$$E_z/H > eI/Mc^2 \equiv (E_z/I)_{\text{cr}} \quad (13)$$

After several cyclotron half-cycles, the deuterons acquire an energy

$$\mathcal{E} \sim l \mathcal{E}_L \left(\frac{E_z}{H} \right)_{\text{cr}} \sim l \frac{e^2 I^2}{Mc^4}; \quad l = 1, 2, 3 \dots \quad (14)$$

Thus, the minimal energy $\mathcal{E} \sim 5 \times 10^{-7} I^2$ amounts to $\sim 5 \times 10^4 \text{ eV}$ for a CP and $\sim 5 \times 10^5 \text{ eV}$ for a PF, which agrees with the experiments.¹⁻³ Moreover, the values $l = 1, 2, \dots$ in (14) apparently correspond to the deuteron energy-spectrum peaks registered in Ref. 3.¹²

The time of formation of the accelerated deuteron should be

$$\tau_{\text{theor}} \sim \pi l_{\text{max}} / \omega_{Hi} \sim 3 \cdot 10^{-3} l_{\text{max}} r / I. \quad (15)$$

Substituting the upper bound of the measured energies of the deuterons in (14), we get $l_{\text{max}} \sim 10$. From (15) we then get $\tau_{\text{theor}} \sim 10^{-7} \text{ sec}$, for typical CP parameters and $\tau_{\text{theor}} \sim 10^{-8} \text{ sec}$ for PF, which agrees with the experimental results.^{1,3}

6. CONCLUSION

1. It is shown in the present paper that a spectroscopic investigation reveals the development, in a Z pinch, of low-frequency noise with field intensity $F_0 \gtrsim 50 \text{ kV/cm}$. A polarization analysis had established that the low-frequency noise constitutes apparently Bernstein modes. This suggests a new possible explanation of the mechanism of ion acceleration under conditions when the current velocity

$$u \gtrsim (eI v_{Te}^3 / Mc^2)^{1/8} \equiv u_2$$

is reached [this is equivalent to the inequality (13)].

We note that $u_2 \gtrsim u_1$, with $u_2/v_{Te} \approx 5 \times 10^{-2} I^{1/4} T^{-1/8} \approx 0.5$. A kinetic calculation³⁰ has shown that in a rarefied corona (in the periphery of the pinch) with concentration $N(r) \lesssim 10^{-2} N(0)$ the velocities reached can be even $u > v_{Te}$. Of course, certain definitely that values $u \sim u_2$ are reached it is necessary to carry out kinetic calculations of a Z pinch with allowance for anomalous transport phenomena due to the Bernstein modes, as well as to perform new experiments.

From the theoretical point of view, observation of Bernstein modes is not surprising, inasmuch as at $v_{Te} > u \gtrsim v_{Te} (m/M)^{1/4}$, out of all the instabilities possible in Z pinches, according to Ref. 26, the Bernstein modes are characterized by the largest growth rate¹³ $\gamma \lesssim \omega_{He} (m/M)^{1/4}$.²⁸

2. It is of interest to compare the critical value of the conduction field E_z or of (13) with the theoretical estimate of the low-frequency noise F_0^{theor} from Sec. 5. It turns out that $E_z / F_0^{\text{theor}} \sim (u_2/v_{Te})^{5/2} < 1$. Therefore the profiles of the Balmer lines are determined principally by the low-frequency noise fields.

We emphasize that both the measured and theoretically estimated low-frequency noise field does not exceed at the instant of the first singularity $F_0(t_1)$ the field of the low-frequency noise at the instant of the second singularity $F_0(t_{II})$. At first glance this contradicts the data on the time scan of the Z -pinch emission, which show that at the instant t_1 the wings of the Balmer lines can be traced farther (in terms of $\Delta\lambda$) than at the instant T_{II}). Actually, the scan data are explained by the

fact that the absolute intensity of the Balmer lines at the instant t_{II} is relatively less than at the instant t , for at least two reasons. First is the increase of the temperature: $T_e(t) \ll T_e(t_{II}) \sim 10^2$ eV (for the CP). The second is the difference between the dynamics of the neck of the pinch near the instants t_I and t_{II} . Near the instant t_I there is no substantial leakage of plasma out of the neck region, inasmuch as with increasing voltage breakdown through the gas near the wall takes place apparently even during the initial stage of its development. This breakdown shunts the neck and stops temporarily the contraction of the pinch.¹⁴ Near the instant t_{II} , the outflow of the plasma from the neck is quite substantial; according to the MHD calculations³⁰ the running number of particles can decrease by two orders of magnitude.

3. In the present investigation of the Z pinch we have observed also Langmuir noise with amplitude $E_0 \sim 50-80$ kV/cm. This exceeds by one order of magnitude the thermodynamic equilibrium value $E_{0t}^{\text{theor}} \sim 3 \times 10^{-11} N^{3/4} T^{-1/4} \sim 2-3$ kV/cm.

The assumption that Langmuir noise exists in a PF was advanced already by Gribkov *et al.*³⁷ to explain the anomalous scattering of light in the skin layer. Investigation of the radiation of a PF at the frequency $2\omega_p$ also offered evidence of the presence of Langmuir noise at above-thermal level.³⁸ Nonetheless, the origin of the Langmuir noise and their role in the dynamics of the Z pinch can serve as the subject of further theoretical and experimental research.

The authors are deeply grateful to academician M. A. Leontovich for interest in the work, and also to S. Yu. Luk'yanov and V. S. Lisitsa for helpful discussions.

¹⁾By half-width is meant here and elsewhere the full width at half maximum of intensity.

²⁾Dips at distances λ_v will be called for brevity v dips ($v = \alpha$ or β).

³⁾Dips due to the resonant dependence of Γ_v on the detuning were "rediscovered" by Lee¹⁷ four years after the publication of our paper.⁸ We indicate also that in his paper Lee took into account neither the multilevel structure of the atom nor the microfields of the ions, although these factors play an important role for hydrogen lines and were included in consideration in our earlier papers.^{8,11}

⁴⁾For this reason, the observed profiles could likewise not be attributed to combined Stark-Zeeman effect. In addition, this splitting depends substantially on the angle between H and F.²⁰ It is doubtful therefore that after averaging over the direction and magnitude of the vector F there remains such a rough structure as observed in the present experiment.

⁵⁾We emphasize also that the adiabatic satellites cannot lead to such abrupt drops of the intensity as the nonadiabatic mechanism of the action of the HF noise: $\Delta S_{\text{sat}}/\Delta S_{\text{dip}} \sim [\min(\epsilon_v, \gamma_p)/\omega_p]^2 \ll 1$.

⁶⁾Recently Piel and Richter²¹ have shown that numerous weak peaks observed by them on the H_β line can likewise not be traditionally interpreted as adiabatic satellites and are apparently molecular H_2 lines. Inasmuch as in the present experiment it turned out that the distance from the center of the D_γ line to the observed singularity depends on the pressure of the molecular deuterium ($\propto P_0^{1/2}$), these singularities are not molecular D_2 lines. This conclusion is confirmed also by a check with the aid of the tables of Ref. 22, which has shown that there is no one-to-one correlation between the positions of the D_2 lines and the observed singularities on the profiles of D_α , D_β , and D_γ . We note incidentally that the experiment of Piel and Richter²¹ was initiated by an idea of Drawin and Ramette²³ that the singularities on the profiles of HeI can be attributed to the molecular lines of He₂. This idea, however, was not confirmed.²⁴

⁷⁾Here and below, in all the practical formulas the wavelength is measured in Å, the electric field intensity in kV/cm, the temperature in eV, the current in Å, the plasma concentration in cm^{-3} , and the pinch radius in cm.

⁸⁾In the derivation of (10) we took into account the fact that the linear dimension of the volume that is imaged on the monochromator slit exceeds the minimum radius of the pinch, and averaging was carried out over the angle in the (r, φ) plane.

⁹⁾We have shown²⁵ that the "blue" asymmetry noted in Fig. 7c denotes a characteristic radial velocity $v_r \sim 2 \times 10^7$ cm/sec or an effective temperature $T_e \sim 300$ eV (at $t \sim t_{II}$).

¹⁰⁾The assumed development of Bernstein modes can also explain the results of an experiment²⁷ in which the profiles of the Balmer lines from H_α to H_ϵ , in observations along the axis of the Z pinch, turned out to be much broader than in observations across the axis.

¹¹⁾These shortcomings were noted by the authors of Ref. 31 themselves.

¹²⁾The nonmonotonic character of the deuteron energy distribution curve in the region of high energies was noted already in an area experiment.²

¹³⁾Filippov's recently reported experiments³³ offer additional (albeit indirect) evidence favoring the presence of Bernstein modes in a Z pinch. They have established that in a PF a reconnection of magnetic force lines takes place, with formation of a neutral current sheath. According to an idea of Syrovatskii,³⁴ in the course of decay of the current sheath plasma turbulence is developed and fast particles are generated. Babykin *et al.*,³⁵ who investigated experimentally the annihilation of opposing magnetic fields, succeeded in identifying a low-frequency plasma turbulence with Bernstein modes.

¹⁴⁾We refer here to cases when the initial electric field intensity in the discharge tube is $E_z(0) \leq 0.2-0.3$ kV/cm. When $E_z(0)$ is increased to 1.5-2.5 kV/cm, the neutron pulse, as is well known, begins to appear already at the instant t_I .³⁶ This indicates that in the latter case the concentration of the neutrals near the wall is substantially decreased and this hinders the breakdown.

¹⁵⁾S. Yu. Luk'yanov, Goryachaya plazma i upravlyaemyi yadernyi sintez (Hot Plasma and controlled Nuclear Fusion), Ch. XI, Nauka, 1975.

¹⁶⁾B.G. Brezhnev, *Izv. Akad. Nauk SSSR, OTN, energetika i avtomatika* 2, 54 (1960).

¹⁷⁾N.V. Filippov *et al.*, 8th Eur. Conf. on Contr. Fusion and Plasma Phys. 1, 63 (Prague, 1977). N.V. Filippov and T.I. Filippova, *Pis'ma Zh. Eksp. Teor. Fiz.* 25, 262 (1977) [JETP Lett. 25, 241 (1977)]

¹⁸⁾I.F. Kvaratskhava, Yu.V. Matveev, and N.G. Reshetnyak, *Pis'ma Zh. Eksp. Teor. Fiz.* 15, 619 (1972) [JETP Lett. 15, 437 (1972)]

¹⁹⁾I.G. Persiantsev, V.D. Pis'mennyi, A.T. Rakhimov, and A.M. Starostin, *Pis'ma Zh. Eksp. Teor. Fiz.* 16, 68 (1972) [JETP Lett. 16, 45 (1972)]

²⁰⁾S.K. Zhdanov and B.A. Trubnikov, *Pis'ma Zh. Eksp. Teor. Fiz.* 28, 61 (1978) [JETP Lett. 28, 55 (1978)]

²¹⁾G.V. Sholin and E.A. Oks, *Dokl. Akad. Nauk SSSR* 209, 1318 (1973) [Sov. Phys. Doklady 18, 254 (1973)]

²²⁾E.A. Oks and G.V. Sholin, *Zh. Eksp. Teor. Fiz.* 68, 974 (1975) [Sov. Phys. JETP 41, 482 (1975)]

²³⁾E.A. Oks and G.V. Sholin, *Zh. Tekh. Fiz.* 46, 254 (1976) [Sov. Phys. Tech. Phys. 21, 144 (1977)]

²⁴⁾E.A. Oks and G.V. Sholin, *Opt. Spetkrosk.* 42, 761 (1977) [Opt. Spectrosc. 42, 434 (1977)]

²⁵⁾A.I. Zhuzhunashvili and E.A. Oks, *Zh. Eksp. Teor. Fiz.* 73, 2142 (1977) [Sov. Phys. JETP 46, 1122 (1977)]

²⁶⁾E.A. Oks, *Pis'ma Astron. Zh.* 4, 425 (1978) [Sov. Astron. Lett. 4, 223 (1978)]

²⁷⁾A.B. Underhill and J.H. Wadell, *Nat. Bur. Stand. Circ. No.* 603 (1959).

²⁸⁾I.I. Rabi, *Phys. Rev.* 51, 652 (1937).

²⁹⁾D.I. Blokhinzev, *Phys. Z. Sow. Union* 4, 501 (1933).

³⁰⁾V. Lifshitz, *Zh. Eksp. Teor. Fiz.* 53, 943 (1967) [Sov. Phys. JETP 26, 570 (1967)]

³¹⁾R.W. Lee, *J. Phys. B.* 12, 1165 (1979).

³²⁾V.V. Aleksandrov, A.I. Gorlanov, N.G. Koval'skii, S.Yu. Luk'yanov, and V.A. Rantsev-Kartinov, in: *Diagnostika plazmy (Plasma Diagnostics)*, No. 3, Atomizdat, 1973, pp. 79, 200.

³³⁾V.V. Aleksandrov, N.G. Koval'skii, S.Yu. Luk'yanov, and V.A. Rantsev-Kartinov, and M.M. Stepanenko, *Zh. Eksp. Teor. Fiz.* 64, 1222 (1973) [Sov. Phys. JETP 37, 622 (1973)]

³⁴⁾Nguyen-Hoe, H.W. Drawin, and L. Herman, *J. Quant. Spectr. Rad. Transfer* 7, 429 (1967).

³⁵⁾A. Piel and H. Richter, *Z. Naturforsch.* 34a, 516 (1979).

³⁶⁾H.M. Crosswhite, *The Hydrogen Molecular Wavelength Tables of G.H. Dieke*, Wiley Intersci., 1972.

³⁷⁾H.W. Drawin and J. Ramette, *Zs. Naturforsch.* 33a, 1285 (1978).

³⁸⁾F. Pinnekamp, *ibid.* 34a, 529 (1979).

³⁹⁾E.A. Oks and V.A. Rantsev-Kartinov, IAE Preprint 3161 (1979).

⁴⁰⁾V.V. Vikhrev and V.M. Korzhaniin, *Fiz. Plazmy* 4, 735 (1978) [Sov. J. Plasma Phys. 4, 411 (1978)].

⁴¹⁾A.N. Babin, S.Yu. Luk'yanov, A.B. Severnyi, G.G. Sidorov, V.I. Sinitin, and N.V. Steshenko, *Izv. KrAO (Bull. Crimean Observ.)* 27, 52 (1962).

⁴²⁾D.G. Lominadze, *Tsiklotronnye volny v plazme (Cyclotron Waves in Plasma)*, Ch. 2, Metsniereba, Tbilisi, 1975.

- ²⁹V.F. D'yachenko and V.S. Imshennik, in: *Voprosy teorii plazmy (Problems of Plasma Theory)*, No. 8, Atomizdat, 1974, p. 164.
- ³⁰N.M. Zueva, V.S. Imshennik, O.V. Lokutsievskii, M.S. Mikhailova, Preprint, *Inst. Appl. Mech., USSR Acad. Sci.*, No. 73, (1975).
- ³¹V.S. Imshennik, S.M. Osovets, and I.V. Otroshchenko, *Zh. Eksp. Teor. Fiz.* **64**, 2057 (1973) [*Sov. Phys. JETP* **37**, 1037 (1973)]
- ³²L.D. Landau and E.M. Lifshitz, *Teoriya Polya (Classical Theory of Fields)*, Nauka, 1967, § 22 [Pergamon].
- ³³N.V. Filippov, *Pis'ma Zh. Eksp. Teor. Fiz.* **31**, 131 (1980) [*JETP Lett.* **31**, 120 (1980)]
- ³⁴S.I. Syrovatskiĭ, in: *Problemy solnechnoi aktivnosti i kosmicheskaya sistema "Prognoz"* (Problems of Solar Activity and the Cosmic System "Prognoz"), Nauka, 1977, p.5.
- ³⁵M.V. Babykin, A.I. Zhuzhunashvili, E.A. Oks, V.V. Shapkin, and G.V. Sholin, *Zh. Eksp. Teor. Fiz.* **65**, 175 (1973) [*Sov. Phys. JETP* **38**, 86 (1973)]
- ³⁶L.A. Artsimovich, *Upravlyaemye termoyadernye reaktzii (Controlled Thermonuclear Reactions)*, Fizmatgiz, 1963, § 5.4.
- ³⁷V.A. Gribkov, O.N. Krokhin, G.V. Sklizkov, N.V. Filippov, and T.I. Filippova, *Tr. FIAN* **85**, 193 (1976).
- ³⁸R.F. Post and T.S. Marshall, *Phys. Fluids* **17**, 452 (1974).

Translated by J. G. Adashko